The Journal of Chemical Physics

Flow-induced voltage generation by moving a nano-sized ionic liquids droplet over a graphene sheet: Molecular dynamics simulation

Cite as: J. Chem. Phys. **144**, 124703 (2016); https://doi.org/10.1063/1.4944611
Submitted: 21 July 2015 . Accepted: 09 March 2016 . Published Online: 24 March 2016

Qunfeng Shao, Jingjing Jia, Yongji Guan, Xiaodong He, and Xiaoping Zhang

Flow-induced voltage generation by moving a nano-sized ionic liquids droplet over a graphene sheet: Molecular dynamics simulation

Qunfeng Shao, Jingjing Jia, Yongji Guan, Xiaodong He, and Xiaoping Zhang[a)]
Institute of Modern Communication, School of Information Science and Engineering, Lanzhou University, Lanzhou 730000, People's Republic of China

(Received 21 July 2015; accepted 9 March 2016; published online 24 March 2016)

In this work, the phenomenon of the voltage generation is explored by using the molecular dynamics simulations, which is performed by driving a nano-sized droplet of room temperature ionic liquids moving along the monolayer graphene sheet for the first time. The studies show that the cations and anions of the droplet will move with velocity nonlinearly increasing to saturation arising by the force balance. The traditional equation for calculating the induced voltage is developed by taking the charge density into consideration, and larger induced voltages in μV-scale are obtained from the nano-size simulation systems based on the ionic liquids (ILs) for its enhanced ionic drifting velocities. It is also derived that the viscosity acts as a reduction for the induced voltage by comparing systems composed of two types of ILs with different viscosity and temperature. © *2016 AIP Publishing LLC.* [http://dx.doi.org/10.1063/1.4944611]

I. INTRODUCTION

The phenomenon of flow-induced voltage can be potentially applied in nano-scaled self-powered devices that offer much promise for nanotechnology in nano-electromechanical systems (NEMSs) in pursuit of realizing bio-molecular sensing and remote controlling.[1] On the basis of theory proposed by Král and Shapiro,[2] several physical mechanisms have been proposed about induced voltage generation from electrolyte or polar liquids flowing over carbon nanomaterials, such as phonon drag,[2] surface ion hopping,[3] and so on. Meanwhile, a mount of experimental and simulation studies[2–13] have been presented over the past decade. In 2003, Ghosh *et al.* observed that induced voltages were generated in the immersed single-walled carbon nanotubes (SWCNTs) along the direction of flowing water, HCl solution, methanol, and glycerol, which were increased with the flow velocity increasing to saturation.[4,5] The same phenomena were also found in the multi-walled carbon nanotubes (CNTs) and the effect of ions concentration on the induced voltage was demonstrated experimentally.[7] Moreover, not only in CNTs, it was also shown that an induced voltage can be generated from flowing liquids over graphene. Dhiman *et al.* found that 25 mV induced voltage was produced from a $\sim 30 \times 16$ μm^2 sized graphene film surrounded by four patterned electrodes in the 0.6M HCl solution, which was the order of magnitude higher as compared to aligned multiwalled-CNTs in the same solution.[8] Yin *et al.* pointed that the induced voltages ranging from a few to over a hundred millivolts in the HCl water[9] and found that a waving potential up to 0.1 V was arisen from ionic solutions flowing over graphene.[11] Soon after, it was reported that a moving droplet of sea water or ionic solution could induce a few millivolts voltage over a strip of monolayer graphene under ambient conditions.[12] It was found that a pseudocapacitor was formed at the droplet/graphene interface, which gave rise to an electric potential that was proportional to the velocity and dependent on the ions concentration and ionic species of the droplets solutions, and decreased sharply with the increasing number of the graphene layers.

In view of the defects such as volatile, virose, caustic, and thermal dependent of commonly used HCl solution, H_2O and methanol aqueous solutions, etc., that are applied in the studies mentioned above, room temperature ionic liquids (RTILs) show environmentally friendly, healthily safe, and high thermosteady so that they can be potentially used as extraordinary electrolyte in extreme conditions and also are harmless to environment and human beings when applied to NEMSs in biomedical areas. Moreover, nano-sized droplet employed in NEMSs presents strong surface effect which enhances the droplet surface and benefits the induced voltage generation. Here, the flow-induced voltage generation from a nano-size imidazole ionic liquids (ILs) droplet moving along the monolayer graphene sheet is explored by using the effective method molecular dynamics (MD) simulations for the first time. The research results indicate that induced voltages can be generated from the movement of an imidazole ILs droplet on the monolayer graphene sheet. According to the simulation results, we attribute the similar saturation of the ionic drifting velocity to the force balance of the liquid droplet that have not been made clear explanations so far. Taking the Coulombic interactions and the opposite direction Coulombic interactions between graphene charge carriers and cations and anions adjacent to the graphene surface into consideration, by involving the distribution of the charge density in z direction, we develop the advanced equation to replace the traditional equation referring to the mechanism of surface ion hopping. From the developed equation, the similar increase to saturation of the induced voltage with the applied velocities increasing is

a)Author to whom correspondence should be addressed. Electronic mail: zxp@lzu.edu.cn.

obtained and a larger output power ~365 nW can be generated from the [EMIM][BF_4] droplet system for the same size level as HCl solution of Dhiman *et al.*[8] with velocity ~0.01 m/s at 300 K. Furthermore, it is found that the higher viscosity of the ILs weakens the flow induced voltage for the bigger viscosity resistance. It is believed that the results presented below should be of great value to develop nano-devices based on liquids in NMES.

II. MOLECULAR MODEL AND SIMULATION DETAILS

MD simulations of two kinds of imidazole ILs [EMIM][BF_4] and [EMIM][PF_6] droplets, respectively, moving on a strip of monolayer graphene sheet under an acceleration are performed by using the DL_POLY4.04 package.[14]

Fig. 1 shows diagrams of the simulation models, where geometry structure of single molecules of [EMIM][BF_4] and [EMIM][PF_6] with atom labels noted is displayed in Fig. 1(a) and the simulation models shown in Fig. 1(b) are an [EMIM][BF_4] droplet on a strip of monolayer graphene. The monolayer graphene sheet is constructed with 2450 carbon atoms with dimension of 86.4×74.6 Å^2 which is kept frozen to prevent the graphene from shifting during the MD simulations. The 512 [EMIM][BF_4] ion pairs are initially stacked in a simple spherical structure to construct a droplet by use of the PACKMOL software, where the model structure of the single IL pair is derived from the Cambridge Crystallographic Data Centre (CCDC). Equilibration was obtained by performing series of MD simulations with the Nosé-Hoover thermostat from 50 K up to 300 K gradually within 6 ns, after that density of the [EMIM][BF_4] droplet is about 1.226 g/cm^3 at 300 K that is about 4% error compared with 1.283 g/cm^3 at 298.63 K.[15] The whole model of the droplet on the monolayer graphene is always at the center of the simulation box that is $86.4 \times 74.6 \times 150$ Å^3 in size and periodic boundary conditions are employed in the whole MD simulations. And the other simulation model is built just with the 512 [EMIM][BF_4] ion pairs replaced by 512 [EMIM][PF_6] ion pairs as Fig. 1(b).

For the MD simulation, the non-polarizable force field of ILs employed is based on the systematic all-atom force fields (AA-FFs) developed by the work of Canongia Lopes and Pádua[16] that is in the frame of optimized potential for liquid simulation/all atom (OPLS-AA) force field,[17,18] which is a combination of parameters derived from quantum chemical calculations and force fields published in the literature. Its potential energy's functional expression is

$$\begin{aligned} U &= U_{bonds} + U_{angles} + U_{dihedrals} + U_{nonbond} \\ &= \sum_i \frac{1}{2} k_r (\mathrm{r} - \mathrm{r}_0)^2 + \sum_i \frac{1}{2} k_\theta (\theta - \theta_0)^2 \\ &\quad + \sum_i V_n [1 + \cos(\mathrm{n}\phi - \gamma)] \\ &\quad + \sum_i \sum_{j>i} \left\{ 4\varepsilon_{ij} \left[\left(\frac{\sigma_{ij}}{r_{ij}}\right)^{12} - \left(\frac{\sigma_{ij}}{r_{ij}}\right)^{6} + \frac{1}{4\pi\varepsilon_0} \frac{q_i q_j}{r_{ij}} \right] \right\}, \end{aligned}$$

where the total energy of the given system is the sum of bond stretch, bond angle bend, dihedral torsion, and pairwise nonbonding energies concluding the van der Waals (vdW) interactions computed by the Lorentz-Berthelot rules, and Coulombic interaction of partial atomic charges. The Tersoff–Brenner covalent potential[19–21] that had been the successfully described mechanical properties of carbon nanotubes[22] is used to describe the interaction between the carbon atoms of the graphene sheet, parameters shown in Table I.[21] The vdW and the real space electrostatic interactions are truncated and shifted to zero at 12 Å.

First, MD simulations of the whole system including [EMIM][BF_4] droplet and the monolayer graphene sheet are performed in the NVT ensemble at temperature 300 K using the Nosé-Hoover thermostat with a relaxation time constant of 1.0 ps. After 5 000 000 steps for the 1.0 fs time step, total energy of the system with time steps is shown in Fig. 2, which reveals that the system reached an equilibrium. The motion equations are solved by using the Verlet leap-frog integrator with 1.0 fs integration time step. After equilibration, a series of accelerations ranging from 0.001 Å/ps^2 to 0.003 Å/ps^2 are applied, respectively, on the droplet to collect corresponding datum.

The system structure after 5 ns equilibration was shown in Fig. 3, which is employed as an initial condition for the next simulations. And then, a series of accelerations imposed only along the x direction are, respectively, applied on the droplet to drive it moving over the graphene sheet, which is equivalent to an external force that could be handled more practically in experiments. Next, the similar simulations processing at temperature of 343.15 K are performed to keep the [EMIM][PF_6] as liquid phase, and the [EMIM][BF_4] droplet and the [EMIM][PF_6] droplet moving, respectively, along the same monolayer graphene sheet as at 300 K.

III. RESULTS AND DISCUSSION

It can be visually seen from Fig. 3 that when the system reached equilibrium, more ions were present on the graphene

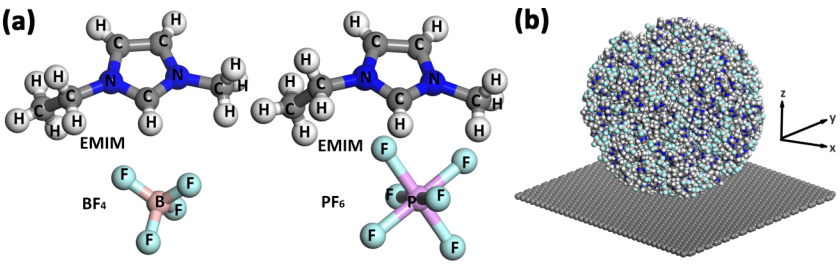

FIG. 1. Geometry structure of [EMIM][BF_4] and [EMIM][PF_6] with atom labels noted in (a) and the simulation model of a droplet of ILs [EMIM][BF_4] placed on a monolayer graphene sheet in (b). Periodic boundary conditions are applied in x, y, and z directions.

TABLE I. Parameters in Tersoff potential for carbon.

Parameter	Carbon
A(kcal)	408.32
B(kcal)	82.86
$\lambda\mu$	3.487 9
μ	2.211 9
β	$1.572\,4 \times 10^{-7}$
n	0.727 51
c	$3.804\,9 \times 10^{4}$
d	4.384
h	−0.570 58
R(Å)	1.80
S(Å)	2.10
χ_{C-C}	1.0

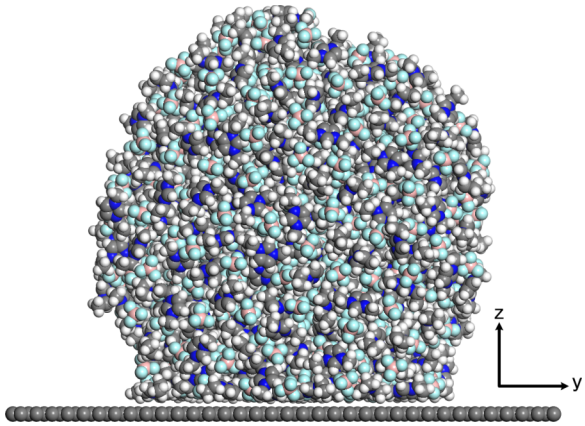

FIG. 3. The cross section of the system structure after 5 ns equilibration.

surface than the non-equilibrium conditions. It is mainly due to the vdW interactions between graphene sheet and IL so that cations and anions are both adsorbed on the monolayer graphene sheet. Fig. 4 shows ions distribution along different directions of the droplet. It can be found from Fig. 4(a) that the distance between the first peak of the cations [EMIM]+ and the graphene surface is ~4.4 Å, which is closer to the graphene surface than the anions BF_4^- ~5 Å. According to Fig. 4(b) that the distribution of cations is basically consistent with that of anions along x direction where the droplet is moving, and also the same distribution in y direction shown as Fig. 4(c). Therefore, only the influence of heterogeneity of charge density distribution along z direction was considered when we calculated the voltage in this work. Based on the simulations results, we estimate the ionic accumulated displacements in each direction and obtain that the displacements in y and z directions are much less than that of in x direction, which indicate when an external force is applied in the x direction, the cations and anions in the droplet will be driven to move on the monolayer graphene sheet both in the x direction.

Fig. 5 presents a nonlinear increase of the cations and anions drifting velocities, respectively, with time under the different applied accelerations at temperature 300 K. The ionic drifting velocity can be estimated by the accumulated displacement. It can be seen obviously that both cations and anions drifting velocity reach saturation after a while of nonlinear increase with time and similar saturation values are reached with different accelerations applied. Upon a steady movement of the droplet on the frozen graphene sheet, it is well known that there is always a viscosity resistance directly proportional to its moving velocity. After applied an acceleration a, the droplet moving velocity increases and the viscosity resistance gradually grows up. When the viscosity is equal to the constant external force developed by acceleration a, the droplet reaches the equilibrium condition of force in its moving direction and keeps a constant velocity as is shown in Fig. 5.

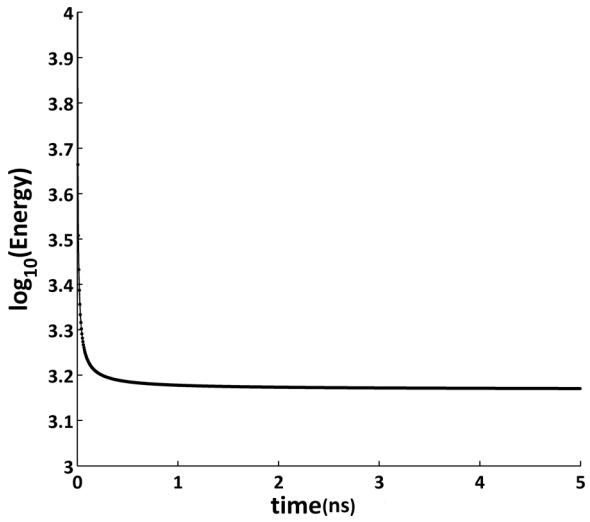

FIG. 2. The variation of total energy with relaxation time steps of [EMIM][BF_4] droplet moving along the monolayer graphene sheet.

This saturation effect shown above is qualitatively similar to previous experiments and MD simulations[3,8,13] and is generally consistent with the mechanism of surface ion hopping,[3] according to which the induced voltage is thus attributed to the velocity of ionic drifting in the flow direction. On the basis of the mechanism of liquid-flow induced voltages, the induced voltages can be estimated by[3]

$$V = RI = R\sigma eL\nu, \tag{1}$$

where $R = \rho L/S$ is the graphene sheet resistance, in which ρ the resistivity of graphene is $10^{-8}\Omega$m, L and S are, respectively, the contact length and the contact area of the droplet with graphene sheet, the range of the average charge carrier density of graphene σ is 10^{19}-10^{20} m^{-2}, e is the electronic charge of 1.6×10^{-19} C, and ν is the anions Cl^- drifting velocity.

Due to the Coulombic interactions between graphene free-charge carries and adsorbed ILs ions, the carriers are dragged along the droplet moving direction, which will create a current. Although the adsorbed cations and anions are drifting in the same direction because of the applied acceleration, the anions drifting leads to a current in the opposite moving direction of the droplet that cancels out or reduces the current flow resulting from the drifting of cations in the droplet moving direction. Furthermore, the Coulombic interactions strength is proportional to the charge and inversely proportional to the distance square, so the effect of the charge density varying in z direction has to be taken into consideration when flow

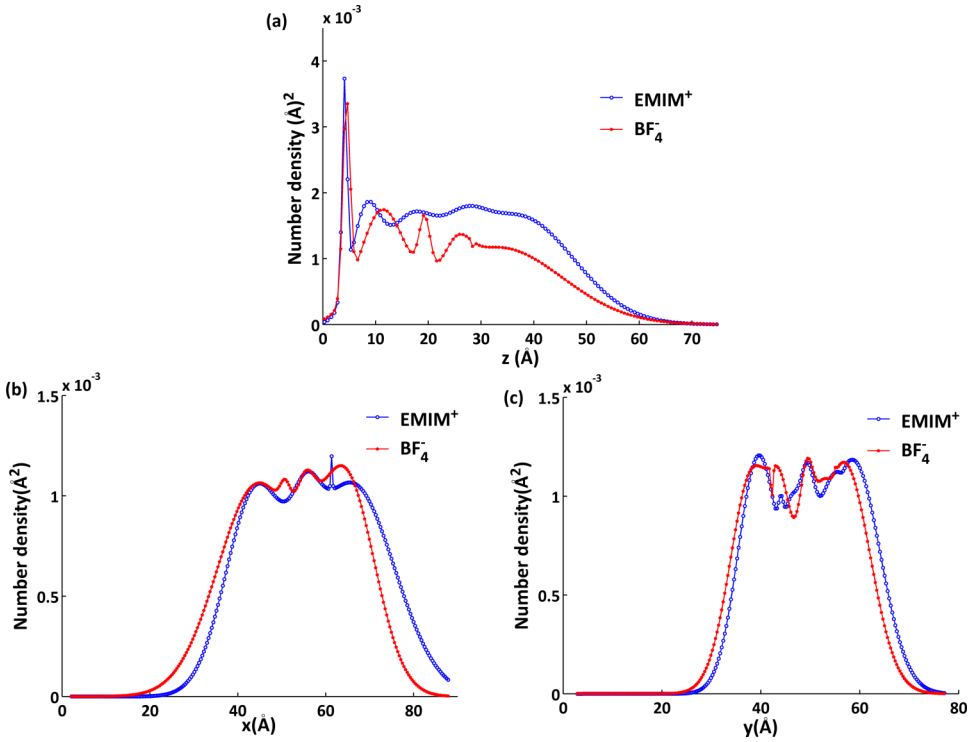

FIG. 4. Ions distribution along different directions of the droplet.

induced voltage is calculated. The distribution of charge density of cations and anions in xy-plane along z direction derived from the simulation results is shown in Fig. 6(a) under the acceleration $a = 0.0025$ Å/ps^2, which is estimated by the summation of every atom's partial charge weighted with the atom's number density along z direction, which is always used to describe the mean number density of the atom in the area at a certain z position. However, the previous studies[8,13] evaluated the voltage according to the anions velocity only due to the weaker interactions between the hydronium ions of HCl solution flow with the graphene; here we estimated the voltage including velocities of anions and cations for the more accurate voltage. Therefore, we develop traditional Eq. (1) as

$$V = RI = R\sigma eL\left(v^+ - \frac{\rho^-}{\rho^+}v^-\right), \tag{2}$$

where the v^+ and v^- are the average drifting velocities of cations and anions, $\frac{\rho^-}{\rho^+}$ is a correction term, and ρ^- and ρ^+ are the first peak of the charge density of cations and anions most adjacent to the graphene sheet surface in z direction considering the inverse relationship between the Coulombic interactions and distance square. According to developed Eq. (2), the induced voltage for the different average charge carrier density of graphene can be calculated and shown in Fig. 6(b) with the acceleration $a = 0.0025$ Å/ps^2; the ρ^- and ρ^+ are 0.0125 and 0.0445, respectively. It can be evidently seen from Fig. 6(b) that voltages ~0.2315-2.315 μV are generated by the relatively small dimension models of the nano-sized polar liquid [EMIM][BF_4] droplet moving along the monolayer graphene sheet at 300 K in our simulations. However, with the bulk liquid 0.6M HCl solution flowing at a velocity of ~0.01 m/s, the output power is ~85 nW for which the system optimal resistance is ~5 KΩ in micro-sized system;[8] if systems

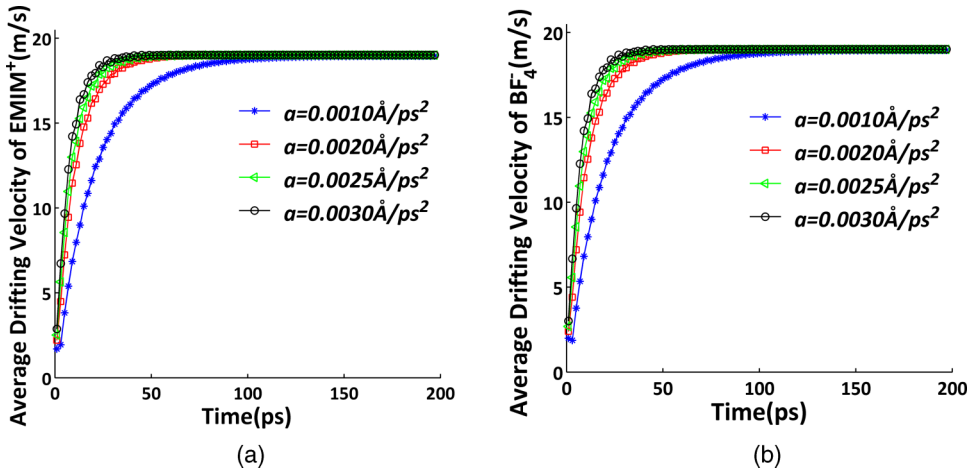

FIG. 5. Average drifting velocities of cations $[EMIM]^+$ in (a) and of anions BF_4^- in (b), varying with time under different applied accelerations in the MD simulation at 300 K.

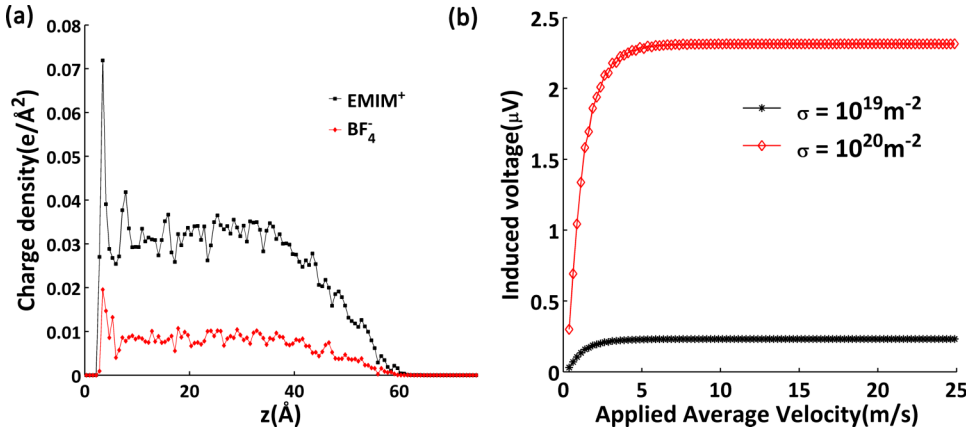

FIG. 6. Under the acceleration $a = 0.0025$ Å/ps^2 at 300 K, (a) shows charge density distribution of cations and anions of [EMIM][BF_4] droplet varying in xy-plane along z direction. (b) shows the induced voltages generated from the [EMIM][BF_4] droplet moving along the monolayer graphene sheet, varying with the applied velocity for the different average charge carrier density of graphene.

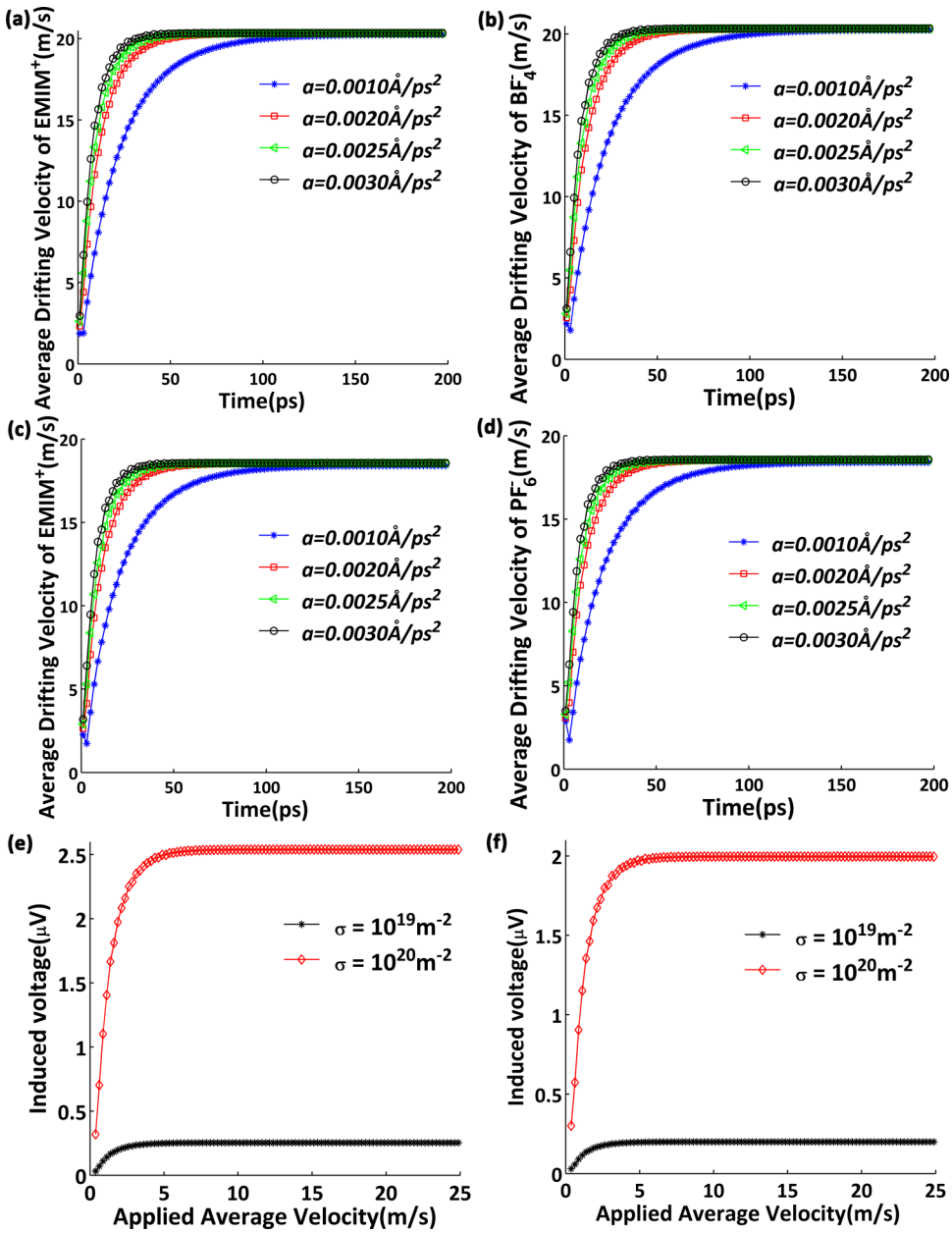

FIG. 7. At 343.15 K, the average drifting velocities of cations $[EMIM]^+$ in (a) and of anions $[BF_4]^-$ in (b) of [EMIM][BF_4] droplet, and the average velocities of cations $[EMIM]^+$ in (c) and of anions $[PF_6]^-$ in (d) of [EMIM][PF_6] droplet. (e) and (f), respectively, show the induced voltages generated from the [EMIM][BF_4] droplet and the [EMIM][PF_6] droplet moving along the monolayer graphene sheet under the acceleration $a = 0.0025$ Å/ps^2, along with the applied velocity for the different average charge carrier density of graphene.

are in the same level, the power ~365 nW is produced by using the imidazole ILs [EMIM][BF_4] droplet in our simulation.

We also perform the same MD simulations of the [EMIM][BF_4] droplet and [EMIM][PF_6] droplet moving along the graphene sheet respectively at temperature 343.15 K, which are applied with the exactly same conditions as 300 K. The model of 512 ion pairs [EMIM][PF_6] droplet is constructed as similar to the [EMIM][BF_4] droplet model in

Fig. 1(b). Following the same simulation procedures, similar results are obtained.

Different ionic drifting velocities and induced voltages are observed with the same applied accelerations on the [EMIM][BF_4] and [EMIM][PF_6] droplets in the same time duration at 343.15 K shown in Fig. 7. The variation trend of the drifting velocities of cations and anions of [EMIM][PF_6] droplet moving at 343.15 K shown in Figs. 7(a) and 7(b) is almost the same as at 300 K; the saturations and the magnitudes are also similar.

But when the saturations are reached, a bit of increase is obtained of the average ionic drifting velocities from the [EMIM][BF_4] droplet moving compared with those of 300 K in Fig. 5. It is mainly because that a higher temperature leads to a lower viscosity, then the viscosity resistance decreases to result in a larger ionic drifting velocity. On the basis of the average ionic drifting velocities, due to the different contact length and areas, and calculated from developed Eq. (2), the corresponding induced voltages are shown in Fig. 7(e) with the acceleration $a = 0.0025$ Å/ps^2. The ρ^- and ρ^+ are, respectively, 0.019 528 and 0.071 898 and the saturation voltages are ~0.254-2.54 μV that is larger than that of 300 K in Fig. 7(b). Figs. 7(c) and 7(d) also show the similar variation of cations and anions saturation drifting velocities of the [EMIM][PF_6] droplet moving at 343.15 K; however, the magnitudes of the saturation velocities are lower than that of [EMIM][BF_4] droplet for its higher viscosity.[23,24] Also, with the ρ^- and ρ^+ as 0.042 74 and 0.192 35 of [EMIM][PF_6] droplet, the saturation voltages are ~0.1997-1.997 μV shown in Fig. 7(f) that is relatively small compared with that of [EMIM][BF_4] droplet in Fig. 7(e). The results further testify that the viscosity acts as a strong reduction to the induced voltages generation for the ILs based models.

IV. CONCLUSION

This work has presented a series of MD simulations of a nano-sized imidazole ILs droplet moving along the monolayer graphene sheet by applying an acceleration on the droplet to drive it moving. The simulation results show that the ionic drifting velocities are increasing to saturation which is caused by the force balance of viscosity resistance and applied external force. Importantly we develop the traditional equation with taking the reversal columbic interactions between the drifting surface ions and the dragged graphene charge carriers and ion density variation along z direction into consideration. From the simulation and calculation results, it is deduced that larger voltages can be generated from our outstanding ILs based models, compared with those systems in the same size of previous experiments and MD simulations, moreover larger the viscosity of ILs smaller the induced voltage. These results may be significant for opening prospects for self-powered NEMS based on ILs under ambient conditions and allow the development of applications in various self-powered nano-devices.

ACKNOWLEDGMENTS

This work is supported by the Fundamental Research Funds for the Central Universities (Nos. lzujbky-2014-46 and lzujbky-2015-306).

[1]Z. L. Wang, Adv. Mater. **24**, 280 (2012).
[2]P. Král and M. Shapiro, Phys. Rev. Lett. **86**, 131 (2001).
[3]B. N. J. Persson, U. Tartaglino, E. Tosatti, and H. Ueba, Phys. Rev. B **69**, 235410 (2004).
[4]S. Ghosh, A. K. Sood, and N. Kumar, Science **299**, 1042 (2003).
[5]S. Ghosh, A. K. Sood, S. Ramaswamy, and N. Kumar, Phys. Rev. B **70**, 205423 (2004).
[6]A. E. Cohen, Science **300**, 1235 (2003).
[7]J. Liu, L. Dai, and J. W. Baur, J. Appl. Phys. **101**, 064312 (2007).
[8]P. Dhiman, F. Yavari, X. Mi, H. Gullapalli, Y. Shi, P. M. Ajayan, and N. Koratkar, Nano Lett. **11**, 3123 (2011).
[9]J. Yin, Z. H. Zhang, X. M. Li, J. X. Zhou, and W. L. Guo, Nano Lett. **12**, 1736 (2012).
[10]S. H. Lee, D. Kim, S. Kim, and C.-S. Han, Appl. Phys. Lett. **99**, 104103 (2011).
[11]J. Yin, Z. H. Zhang, X. M. Li, J. Yu, J. X. Zhou, Y. Q. Chen, and W. L. Guo, Nat. Commun. **5**, 3582 (2014).
[12]J. Yin, X. M. Li, J. Yu, Z. H. Zhang, J. X. Zhou, and W. L. Guo, Nat. Nanotechnol. **9**, 378 (2014).
[13]B. Xu and X. Chen, Phys. Chem. Chem. Phys. **15**, 1164 (2013).
[14]W. Smith, C. W. Yong, and P. M. Rodger, Mol. Simul. **28**, 385 (2002).
[15]J. Klomfar, M. Součková, and J. Pátek, J. Chem. Eng. Data **57**, 708 (2012).
[16]J. N. Canongia Lopes, J. Deschamps, and A. A. H. Pádua, J. Phys. Chem. B **108**, 2038 (2004).
[17]W. L. Jorgensen, D. S. Maxwell, and J. Tirado-Rives, J. Am. Chem. Soc. **118**, 11225 (1996).
[18]G. Kaminski and W. L. Jorgensen, J. Phys. Chem. **100**, 18010 (1996).
[19]J. Tersoff, Phys. Rev. Lett. **61**, 2879 (1988).
[20]J. Tersoff, Phys. Rev. B **39**, 5566 (1989).
[21]W. C. D. Cheong and L. C. Zhang, Nanotechnology **11**, 173 (2000).
[22]B. Faria, N. Silvestre, and J. N. Canongia Lopes, Compos. Sci. Technol. **71**, 1811 (2011).
[23]C. Schreiner, S. Zugmann, R. Hartl, and H. J. Gores, J. Chem. Eng. Data **55**, 1784 (2009).
[24]K. R. Seddon, A. Stark, and M. J. Torres, Clean Solvents **819**, 34 (2002).